

TORUS-TYPE AIRSHIP AIMING AT HIGH AIRWORTHINESS QUALITY

Hisayoshi Suefuku*, Tsugukiyo Hirayama**
Yoshiaki Hirakawa**, Takehiko Takayama**

* Department of Ocean and Space Systems Engineering, Yokohama National University,
79-5 Tokiwadai, Hodogaya-ku, Yokohama, 240-8501 JAPAN

** Faculty of Engineering, Department of Naval Architecture and Ocean Space
Engineering,
Yokohama National University

Keywords: *Airship, TORUS, Next-Generation-Type, High Airworthiness, Mooring*

Abstract

In this paper, we have an aim developing the next-generation-type airship for resolving airworthiness problems especially for mooring condition. For this purpose, we propose the TORUS-TYPE AIRSHIP. The torus-type airship will have the advanced characteristics of airworthiness especially at mooring condition, and have advanced maneuverability especially for movement of any direction(forward, backward, left, right, rotation), but some instability at flight condition are considered.

At first, we designed a simplified torus-type airship model, and carried out towing experiments about aerodynamic characteristics of the model in upper water space of our huge towing tank instead of carrying out experiments in a wind tunnel. By introducing torus-type airship, we will be able to minimize the mooring area, reduce the maximum mooring forces, and in the result prevent the body damage at mooring.

In the second, we developed a 3D Flight-simulation program using the data from the experiment. By using the numerical simulation, we can evaluate the performance of the torus-type airship from various viewpoint including mooring.

1 Introduction

Nowadays, airships that were used in the past are returning again and their use can be expected in areas such as sightseeing, cargo



Fig. 1. (Left) Photo of the conventional type Airship (Right) Image of the proposed Airship

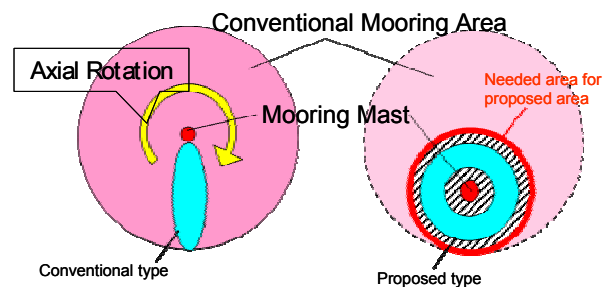


Fig. 2. Difference of the area for needed

transportation, surveillance, disaster prevention and rescue purpose. Left of Fig. 1 is a conventional one (Zeppelin NT). Since the conventional airship requires a large mooring area and facility, landing and taking off from arbitrary place especially from the center of a city are difficult. Of course it is inconvenient for airports far from cities. From this view point, we have room to consider about the shape and related system of airship resolving above problem, other than conventional spindle type airship. we have to discuss that if the most effective shape is spindle or not.

In order to reduce the necessary area by adopting a different shape and mooring system, we propose the following new type of airship.

Our proposal is a Torus shape as the next generation-type airship shown in Fig. 1(Right). As the circular shape has an equi-directional aerodynamic characteristics, its directional control become more easier than conventional ones. This becomes one reason of having high-airworthiness about new airship. The new type airship has following two characteristics.

(1) Effects of wind forces at mooring condition are also equi-directional. So the maximum mooring force become smaller than that of conventional one if the horizontal rotation is not allowed.

(2) The position of mooring system can be set at the center of torus[1][2][3].

So, the area needed for this mooring system become around 1/4 comparing to the area needed for conventional one with the same volume, as shown in Fig. 2.

For evaluating the characteristics at flight condition, dynamical stabilities, including static stabilities, are examined in the following sections.

2 Design of Torus model

2.1 Definition of Torus

We propose Torus-type as a next-generation-type airship. In this paper, simplified-torus type was selected from a view point of construction as shown in Fig. 3 and 4. The surface area S and volume V of simple torus type are given by the following two formula. Present simple model will have relatively large drag in the level flight, but this demerit will be decreased by adopting so called lens type or more flat configuration.

$$S = 2\pi a \times 2\pi b = 4\pi^2 ab \quad (1)$$

$$V = \pi b^2 \times 2\pi a = 2\pi^2 ab^2 \quad (2)$$

2.2 Decision of the model configuration and scale

In this section, the size of the model and the restoring moment for static stability are discussed.

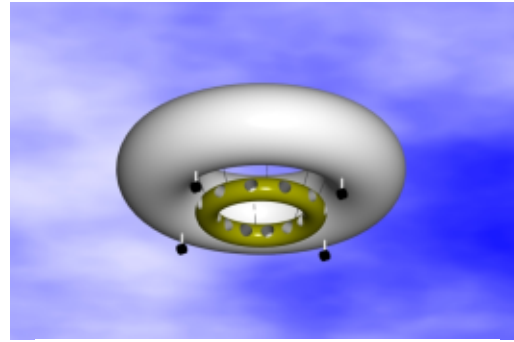


Fig. 3. Simplified torus-type Airship CG

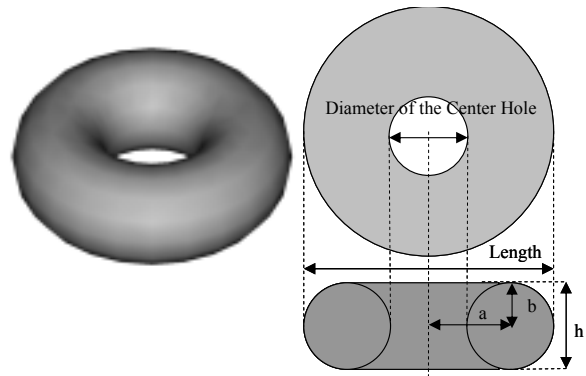


Fig. 4. Torus type (Left) Bird's eye view (Right) Definition

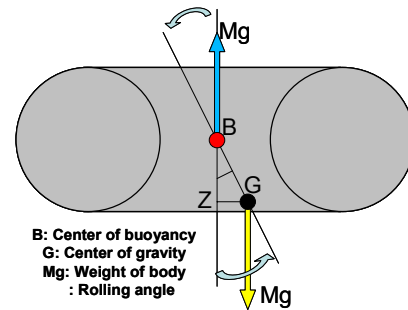


Fig. 5. Restoring moment in rolling same as pitching

2.2.1 Restoring moment

Restoring moment was estimated by formula (3).

$$M_{stability} = Mg \times GZ = Mg \times BG \sin \Phi [Nm] \quad (3)$$

Where BG is the distance between B and G .

2.2.2 Scale of the model

The volume of the actual airship Zeppelin-NT (we call this as the conventional type) is around $8000[m^3]$. Corresponding to this, candidate airship size was varied as shown in Fig.6, fixing the volume as conventional type. Gondola size was also decided referring conventional type. Decided width, height, and length of gondola are 2.7, 2.7, 10.7[m]. Weight of gondola was

estimated as 2000kg. BG was supposed as $\{b(\text{radius of torus tube})+1.35(\text{as a half of the gondola height})\}[\text{m}]$. From the assumed parameters, we examined static stability.

Figure 7 shows the curve of the lever GZ of restoring moment. Maximum GZ become large according to the length become short, because the gondola position become lower. But, in case of 30[m] length, the center hole for mooring and for another equipments disappear. So, we selected the length 35[m] for the present case, especially from view point of minimizing the mooring space.

The scale of model for experiment is decided based on the same as one of supposed airship with length of 35[m] in Table 1. Table 2 shows the candidate scale of Torus model. The model volume is decided having the buoyancy 1.0[kgf] to carry on some device for free-flight test by radio control. From this volume, the torus diameter is decided, and finally the 1/14 scale was selected. Length (or diameter) becomes as 2.5[m]. In addition, two film sheets ($\Phi=1.66[\text{m}]$) are prepared to close the hole of torus model from upper and lower side of the hole. Closing the hole turns it to disk type for checking some aerodynamic influences of the hole of torus.

Table 1. Candidate scale of Torus Type and ZeppelinNT Volume constant

Torus type							
L [m]	b [m]	a [m]	H [m]	Projected Area [m ²]	Surface Area [m ²]	Volum e [m ³]	BG[m]
100.0	2.9	47.1	5.9	580	5452	8000	4.3
80.0	3.3	36.7	6.6	522	4813	8000	4.7
75.0	3.5	34.0	6.9	507	4638	8000	4.8
60.0	3.9	26.1	7.9	460	4057	8000	5.3
40.0	5.2	14.8	10.5	396	3053	8000	6.6
35.0	5.9	11.6	11.8	384	2705	8000	7.3
30.0	7.2	7.8	14.4	388	2217	8000	8.6
ZeppelinNT(Only Hull)							
Length[m]	Diameter[m]	Height with gondola[m]	Frontal Projected Area 154[m ²]	Surface Area [m ²]	Volum e [m ³]	BG[m]	
75	φ14		Projected Area 814[m ²]	2600	8000	8.35	

Table 2. Candidate model scale of Torus type and supposed actual one with Length 35 [m]

Length [m]	b [m]	a [m]	H [m]	Projection Side Area [m ²]	Surface Area [m ²]	Volum e [m ³]
35.00	5.91	11.59	11.83	383.99	2705.2	8000.0
1.75	0.30	0.58	0.59	0.96	6.8	1.0
2.20	0.37	0.73	0.75	1.52	10.7	2.0
2.38	0.40	0.79	0.80	1.77	12.5	2.5
2.50	0.42	0.83	0.84	1.96	13.8	2.9
2.52	0.43	0.84	0.85	2.00	14.1	3.0
2.78	0.47	0.92	0.94	2.42	17.0	4.0
2.99	0.51	0.99	1.01	2.81	19.8	5.0

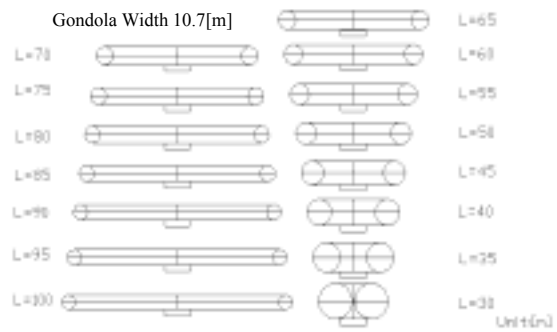


Fig. 6. Candidate profiles of Torus type airship keeping volume constant

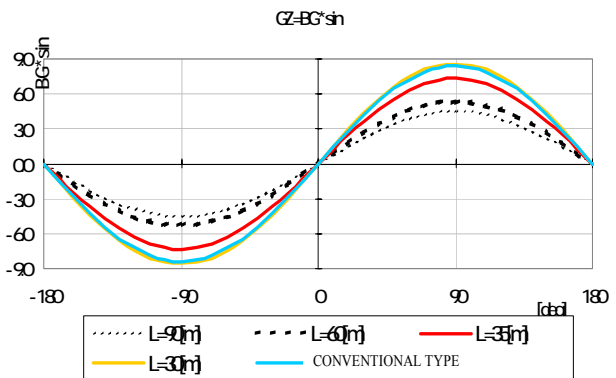


Fig. 7. Curve of GZ according to rolling angle



Fig. 8. Photo of the Torus model

Table 3. Principal dimensions and parameters of the ordered Torus model(Measured)

Measurement Item	Value	Unit
Length	2504	[mm]
Height	904	[mm]
Radius of the Tube	452	[mm]
Diameter of the Center Hole	696	[mm]
Thickness of the body Membrane Materials	0.13	[mm]
Dry Weight	2.30	[kgf]
Volume	3.23	[m ³]
Practical Reserved Buoyancy(contain He gas)	0.97	[kgf]

3 Captured model experiment

3.1 Facility and Device

In a long and large towing tank (100m length, 8m in width) of Yokohama National University, torus-type and disk-type airship was attached to the towing carriage, and the following data were obtained as shown in Fig. 9 and 10: the aerodynamics characteristics of the model, namely drag, lift and moment. About the captured model, the body attitude and the velocity are changed as described in the following section. The results of experiment are used to evaluate the stability of the flight by numerical simulation and forces at mooring condition by static consideration, as shown in chapter 6.

We carried out model experiments utilizing the upper space of huge towing tank of our laboratory, instead of carrying out experiments in a wind tunnel[7]. In the case of a wind tunnel, the wind-generating propeller makes a disturbed flow so some equipment depressing such disturbances are needed. But, in the case of towing tank, model moves in the rested air, so, this condition is very similar to actual flight. The occupied percentage by the sectional area of model to the sectional area of the towing tank (blockage coefficient) is 3.3% (See Fig. 11). It is very small. For these reasons, we consider the result of this experiment is reliable.

3.2 Range of experimental parameters.

This experiment is operated under the following conditions to measure the aerodynamic characteristics of torus type and disk type model.

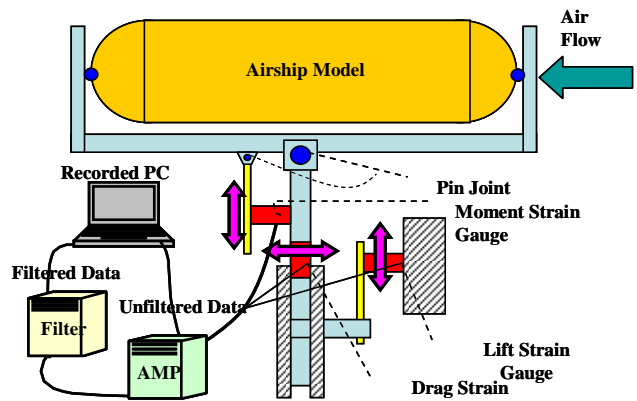


Fig. 10. The measurement instrument from the side view point

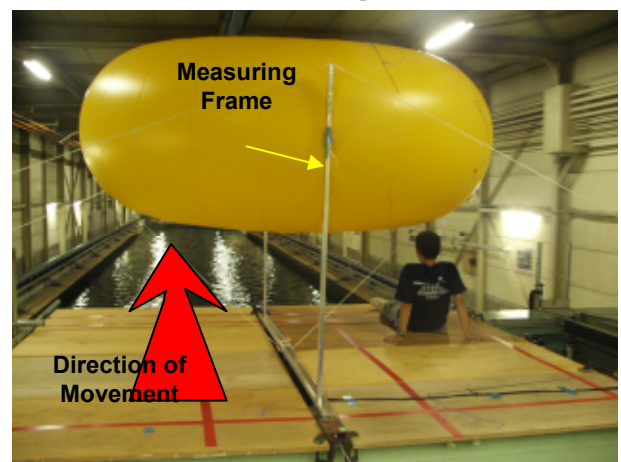


Fig. 11. Photo of torus model supported by measuring frame taken from the backside with a man for comparison

- **Attack angle** of the body
 $-10[\text{deg}] \leq \theta \leq 10[\text{deg}]$
 $(-0.175[\text{rad}] \leq \theta \leq 0.175[\text{rad}])$
 by the step of 5[deg]
- **Clearance** to the ground (colored by green in Fig. 12)
 For measuring the influence of ground effect. The distance between the bottom of model and the upper surface of towing carriage are changed. The clearance are 80[mm], 526[mm],

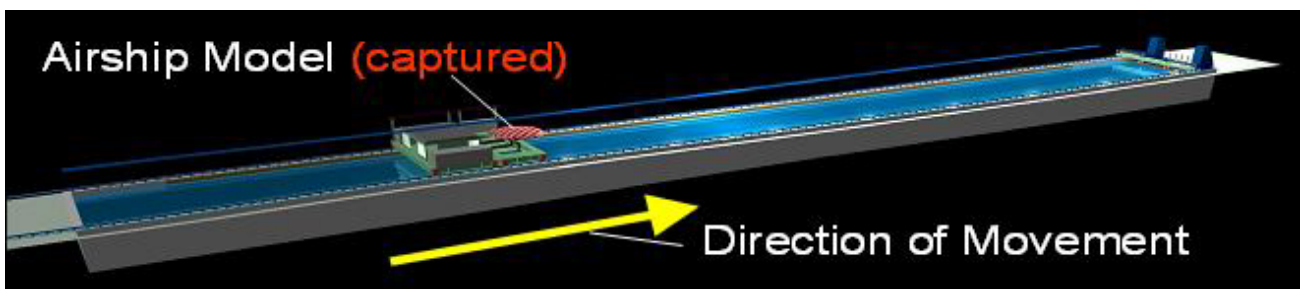


Fig. 9. Towing tank and Experimental apparatus

1026[mm]. The minimum model clearance 80[mm] corresponds to 1.12[m] for supposed actual one, and this is considered as moored condition, excluding gondola height.

- **Speed** of towing carriage
Selected speeds are 1.0[m/s], 1.5[m/s], 2.0[m/s]. Each velocity corresponds to 5.3[m/s], 8.0[m/s], 10.6[m/s] in case of assumed actual airship under the law of similitude of Froude.

- **Distance** between the end of the model and vertical wall of the cabin for measurement experiment

There is a vertical wall after the model end. This is a part of the cabin for drivers of the towing carriage. But the towing carriage for the model is separated, and the distance of vertical wall and the model (colored by yellow in Fig. 12) can be changed. This vertical wall can be considered as a building wall near the mooring cite in the city.

Two conditions are operated. “@Near” means the distance is 1100 [mm], and “@Far” means the distance is 2600[mm] in Fig. 12.

3.3 Reynolds number and Froude number in experiment

Table 4. shows the Reynolds number and Froude number of torus-type model in the

experiment, for the case of torus-type Model in the Experiment and Actual Airship. For comparison, it contains those of the conventional type (Spindle type Zeppelin-NT is quated) under its cruising speed with 22.4[m/s]. Effect of Re on external forces must be considered in case of the estimation of the flight characteristics of actual one.

To consider about the motion characteristic at flight condition of torus-type airship with the same advancing speed of conventional one, the model towing speed must be done at 4.0[m/s], without ground effect, considering the Froude number “Fn”. But the target mission is not the same between conventional one and new one, what is the optimum speed must be considered again for new one.

In the Froude number defined in eq. (4), representative length "l" is airship length.

$$F_n = \frac{V}{\sqrt{gl}} \tag{4}$$

An aerodynamic characteristic including the effect of viscosity depends on Reynolds number (below, abbreviated as Re), but our aim is considering the dynamic motion of torus model. So, Fn is considered as dominant parameter in the law of similitude instead of Re in this paper.

If torus-type airship has a large drag, it need not fly by the same cruising speed as Zeppelin-NT. In case of realizing the same cruising speed as Zeppelin-NT, we must estimate aerodynamic coefficient corresponding to 22.4m/s, by

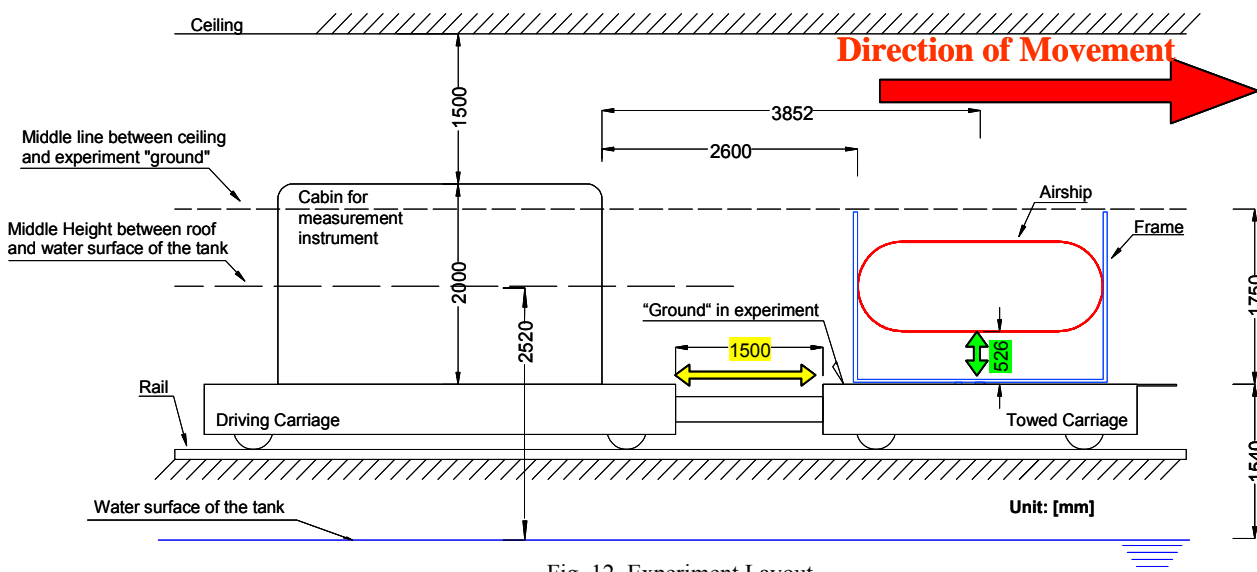


Fig. 12. Experiment Layout

Table 4. Reynolds Number and Fluid Number of each cases in the law of similitude

Torus Model in experiment				
$V_{Model}[m/s]$	1.0	1.5	2.0	4.2
Re	1.6×10^5	2.4×10^5	3.2×10^5	6.7×10^5
Fn	0.2	0.3	0.4	0.8
Actual Torus-type Airship				
$V_{Actual}[m/s]$	3.7	5.6	7.4	16.3
Re	8.3×10^6	1.3×10^7	1.7×10^7	3.7×10^7
Fn	0.2	0.3	0.4	0.8
Actual Conventional Airship(ZeppelinNT)				
$V_{Actual}[m/s]$	5.3	8.0	10.0	22.4
Re	2.5×10^7	3.8×10^7	4.8×10^7	1.1×10^8
Fn	0.2	0.3	0.4	0.8

experiment or CFD method. Before estimating actual ship performances, first, we will complete the simulation for explaining the result of free-flight model experiment. After that, actual ship performances are estimated by estimating actual aerodynamic coefficients based on actual Re.

4 Results of towing experiment

Figure 13, 14, and 15 show examples of obtained results with ground effect: clearance from the bottom of airship to the ground (flat plate) is 80 mm. The case of disk-type is also shown. Disk-type is realized by closing the upper and lower side of center hole of the torus type model by thin film. The experiments shows that the wind force on the moored body will be larger for the torus-type than that of disk-type due to the complex ground effect. On the other hand, for the torus-type a mooring body generate minus lift force and moment for any attitude (attack angle). In addition, the torus-type showed reasonable characteristics in front of vertical wall. Figure 13 shows that drag is decreasing near the vertical wall than far from wall. From these results, it will be said that torus-type has superior characteristics in Lift and Moment coefficient at mooring condition. Moreover, from the estimation of the static wind load on the mooring post and the comparison of this value with the conventional airship (in case of rotation around mooring post is fixed), 34 % decreasing is estimated. By the optimization of the airship configuration, for example by

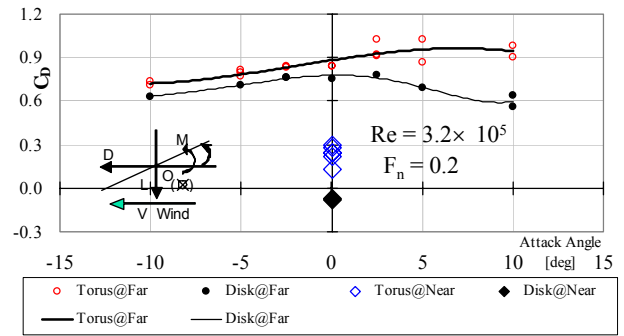


Fig. 13. Experimental results and fitted curve of the Drag coefficient according to attack angle at clearance 80[mm]

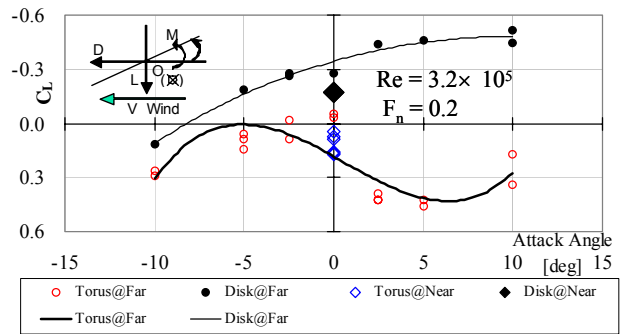


Fig. 14. Experimental results and fitted curve of the Lift coefficient according to attack angle at clearance 80[mm]

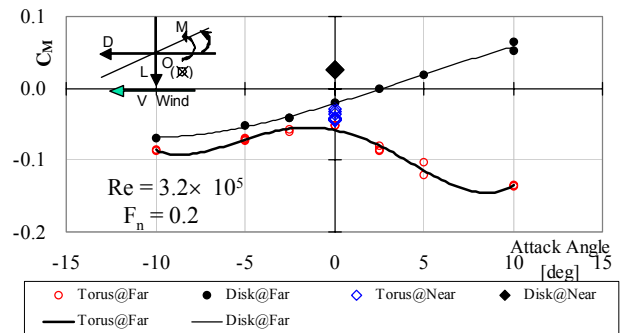


Fig. 15. Experimental results and fitted curve of the Moment coefficient according to attack angle at clearance 80[mm]

adopting lens like configuration, smaller area and smaller load for mooring post will be expected.

5 Free Flight model experiment

As described in introduction, our first point of focusing is about the problem of mooring area. For solving this problem, we proposed a torus-type airship which has a different outdoor mooring system comparing to conventional airship. But the instability of torus-type model on free-flight is predicted easily from the view

point of its shape. We have to examine its motion characteristic by numerical simulations. In case of towing experiment, the measured aerodynamic characteristic is not the one in infinite fluid. So, in numerical simulation, we estimate the aerodynamic characteristics of torus-type from the modified graph based on the results with largest clearance 1026mm, and considering that, without the effect of horizontal plane (correspond to the ground), symmetrical characteristics should appear according to attack angle. From this consideration, it is estimated that the torus type which has the symmetric body show a unique characteristic as follows.

It has a lift to the downward direction in case of small nose-up, and to the upward direction in case of small nose-down as can be seen in Fig. 16. In order to recognize the longitudinal stability characteristics of torus-type model airship with thruster-fan on both sides, radio controlled free flight experiment is carried out. In this experiment no horizontal or vertical fins are equipped. The experiment show an increasing oscillation for the disk-type, therefore the system becomes unstable. For the torus-type, instability is also observed in the pitching direction. But observed constant oscillation is small. Fig. 17 is instantaneous photo, but movie will be introduced at presentation.

6 Evaluation of longitudinal Stability from the point of stability index

For evaluating the longitudinal stability in steady flight, the stability index can be used[3]. For calculating it, moment of inertia I_y in the equation of pitching motion is directly used, instead of using buoyancy (=weight). Equation and definition of coefficients are shown in eq. (5), (6), and (7). After we construct 3D flight numerical simulation for torus-type airship, we consider flight stability also. In this consideration, the tail wings, elevators and rudders are added and NACA0024 wing section are adopted. Results about stability is described in Cap.8.

$$\frac{d^2\theta}{dt} = -\sigma\theta - \delta \frac{d\theta}{dt} \tag{5}$$

$$\sigma_{airship} = \left(-\frac{dC_{MG}}{d\alpha} \frac{1}{2mi^2} \rho V^2 S \bar{c} \right) \tag{6}$$

$$\delta_{airship} = \frac{dC_{Lh}}{d\alpha_h} \frac{l_h^2}{V} \frac{1}{2mi^2} \rho V^2 S_h \tag{7}$$

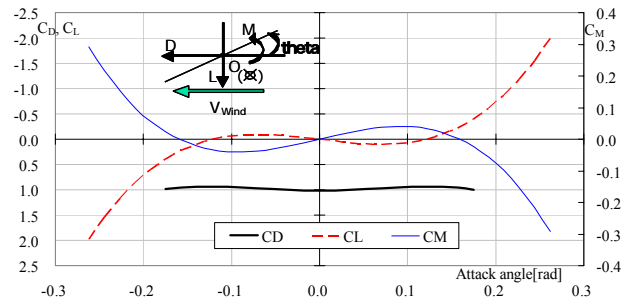


Fig. 16. Estimated aerodynamic characteristic of torus-type at enough altitude without ground effect



Fig. 17. Model for free-flight with propulsion device (small black point on the side)

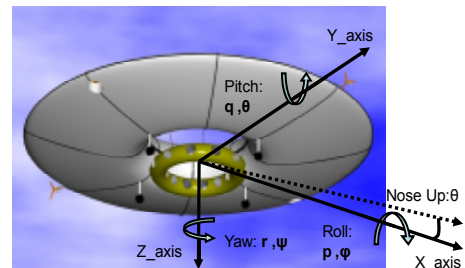


Fig.18. Definition of Numerical simulation (Configuration is not present one but future type)

7 Numerical simulation

For the evaluation of the method of improving the stability and airworthiness of torus-type airship, we develop numerical motion simulation, applying experimental data. Control surfaces, rudder and elevator are also included. It must be noted that fins are not equipped with in case of free flight model experiments. In the

simulation the ground effect can be also considered. In this simulation, position of the center of gravity and position of the center of buoyancy are not the same. But each forces balance. Using the Runge-Kutta method, this program solve the-motion of equations. These equations referring[4][5][6] are shown in the appendix. Definition of motion direction and coordinate systems are shown in Fig.18.

How to estimate the coefficients or derivatives of equation of motions are important matter. Here we referred references [4][5][6] and experimental results .

8 Consideration using simulation

8.1 Decision of a size of tail wings

For the decision of the size of tail wings(here the elevators and rudders are assumed as the same configuration), the simulation is done for the various sizes from 0.6*0.6[m] to 0.8*0.8[m]. Here, we consider the shape of tail wings as square and neglect the inertia effect of the wings .

We carried out loop (vertical turning) simulation with trim or drift angle of 0.3[rad], changing the size of tail wings.

From results in Fig. 19, the appropriate size of wings are selected as 0.64*0.64[m], considering effective and smaller one. in case of the speed (0.89m/s) of free flight model experiment. The size of 0.64*0.64[m] corresponds to 8.4*8.4[m] for actual size. This will be relatively large , because considered speed is very low. But in case of low speed another method of inclining the body will be effective.

8.2 Judgment of the longitudinal stability

Table 5 shows the evaluation of the longitudinal stability from the point of stability index, including the tail wing decided in Sec. 8.1.

Where "G" means good, "NG" means "Not good". NG for small attack angle, seems to corresponds to the free flight experiments without fins described in the section 5.

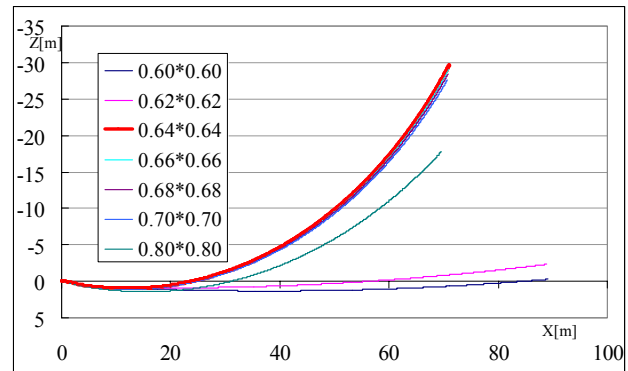


Fig. 19. Trajectories in vertical-plane according to the size of the elevators

Table 5. Evaluation of stability from point of stability index

Attack angle θ [rad]	σ_{airship}	δ_{airship}	Static stability	Damping by tail wings	Evaluation of stability
-0.15	plus	plus	G	G	damped with oscillation
-0.1	plus	plus	G	G	damped with oscillation
-0.05	minus	plus	NG	G	damped without oscillation
0	minus	plus	NG	G	damped without oscillation
0.05	minus	plus	NG	G	damped without oscillation
0.1	plus	plus	G	G	damped with oscillation
0.15	plus	plus	G	G	damped with oscillation

Figure 20 shows the result of simulation changing the given initial disturbances. Those results show no instability comparing to the results in Table 5. This will because that restoring moment is included in numerical simulation, but not in case of calculating stability index. In simulation, initial motion of torus-type model is damped with oscillation.

Anyway, torus type airship show a little longitudinal instability when the center of gravity and the center of buoyancy coincide, but will be recovered by restoring moment and damping force.

8.3 Longitudinal motion

Figure 21 shows the case with PD control of the elevators angle. PD control is represented in eq. 8. Each gains are set "10" in this consideration. When given some disturbances, the body attitude is recovered quickly by elevators. This case , around 20secons corresponds to around 70secons for actual scale. From this result, it will be said that the stable flight will be possible for torus type airship by attaching appropriate control surfaces. Figure 22(left) show the instantaneous motion in animation, with elevators and a rudder. Thrust(drawn as yellow box in fig.) is attached on the mid ship position of both side of the body.

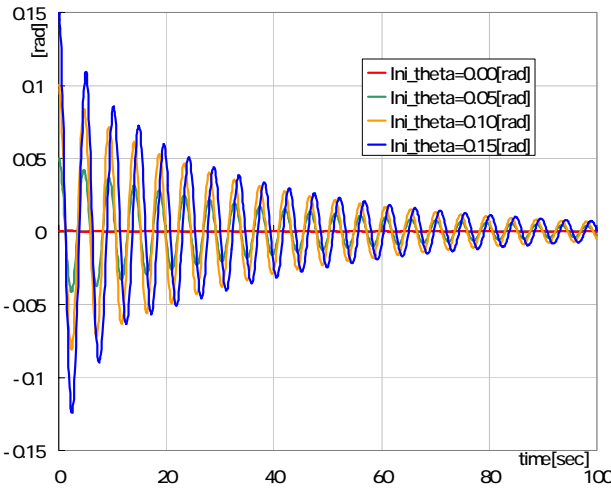


Fig. 20 Response to each disturbances Pitch(Theta)

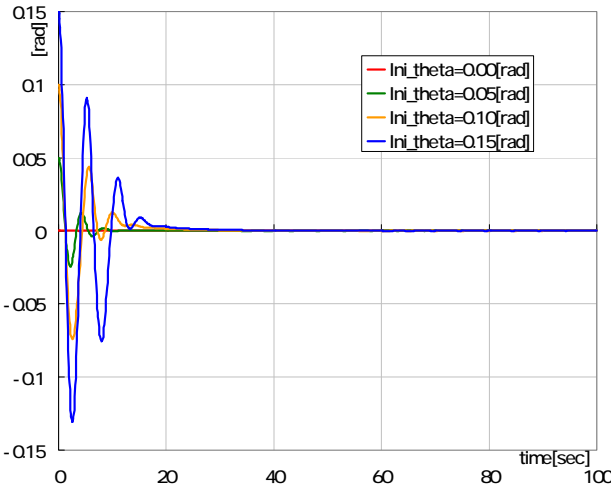


Fig. 21. Response to each initial disturbances Pitch(Theta) under PD control

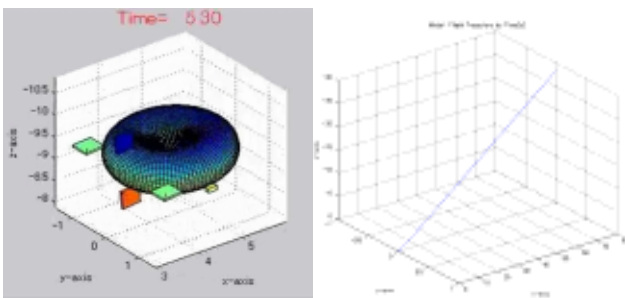


Fig. 22. Numerical simulation
(Left) Model with propulsion device, elevator and rudder
(Right) Trajectory of Model on free-flight

$$\delta_{elevator_input} = -(K_{p_theta}(\theta_{target} - \theta) + K_{d_q}(q_{target} - q)) \quad (8)$$

Constant thrust and parallel thrust direction to body axis is given.

The right figure shows a trajectory of this flight. Each details will be shown in the presentation.

9 Concluding remarks

For resolving the problem of needed area for outdoor mooring of airships, we proposed a new type of airship, namely the torus type. Following characteristics and remarks are obtained.

- (1) About this new type of airship, needed area for outdoor mooring become very small by the one point mooring at the center point of the torus.
- (2) Mooring force become uniform even if the wind direction changed, so the horizontal rotation of the body according to the change of wind direction like conventional airship is not needed. This reduce the number of persons for watching.
- (3) For the confirmation and improvement of high-airworthiness characteristics in mooring and flight condition, we carried out model experiments and numerical simulations, stressing on the longitudinal stability.
- (4) Free flight model experiment showed a little motion instability, but from numerical simulation , this will be depressed by appropriate control surfaces.
- (5) Evaluation of airworthiness characteristics in case of fluctuating external forces , gust wind for example, are needed as the next step.

References

- [1] H.Suefuku, T.Hirayama, Y.Hirakawa, T.Takayama. Basic study on a next-generation type airship with high air-worthiness quality(part1)(in Japanese). *The Japan Society of Naval Architects and Ocean Engineers* , Tokyo Japan, Vol.9E, 2009E-GS4-1, pp131-132, November 2009.
- [2] H.Suefuku, T.Hirayama, Y.Hirakawa, T.Takayama. Study on the Aerodynamic Characteristics and Flight Stability of a Next-generation type Airship with High Airworthiness(in Japanese). *The 41st JSASS Annual Meeting*, Tokyo Japan, JSASS-2010-1116, pp656-659, April 2010.
- [3] H.Suefuku, T.Hirayama, Y.Hirakawa, T.Takayama. Basic study on a next-generation type airship with high air-worthiness quality(part2) (in Japanese). *The Japan Society of Naval Architects and Ocean Engineers*, Tokyo Japan, Vol.10, 2010S-G9-8, pp551-552, June 2010.
- [4] G.A.Khoury, J.D.Gillett. *Airship Technology CAMBRIDGE AEROSPACE SERIES 10*. Cambridge University Press 1999

[5] K.Kato. *Koukuukirikigakunyuumon*. Publication of Tokyo Univ, 2006
 [6] K.Arnstein, W.Klempere Performance of airships . Volume VI of Aerodynamic Theory ,Springer 1936
 [7] Hirayama T.,Miyaji K.,Takayama T.,Hirakawa Y. & Hayashi T. *Evaluation of Landing Flying Boat on the Sea-Development and Applications of a High-Speed Experimental Guiding System- FAST2003, SessionD1,pp83-89, 2003*

Appendix

Symbols in the motion of equation

mg	Gravitational force
B	Buoyancy force
$m_{envelope}$	Mass of envelope
$I_{envelope}$	Moment of inertia of envelope
m_x, m_y, m_z	Added mass
J_x, J_y, J_z	Added moment of inertia
J_{xy}, J_{xz}, J_{yz}	Apparent product of inertia
a_x, a_z	Coordinates of the center of gravity C.G
b_x, b_z	Coordinates of the center of buoyancy C.B
Suffix only "e"	Equilibrium component of each forces and moments
Suffix "E"	component based on earth coordinate system (inertia-system)
Suffix "δe"	component products by the elevators
Suffix "δr"	component products by the rudders
Suffix "δt"	component products by the thrusters

Axial force derivative $\dot{X}_u = \frac{\partial X}{\partial u} u$

The linearized motion equations with small perturbation on body axis as approximation[4]

Axial Force

$$\begin{cases} \frac{dx}{dt} = u \\ \dot{u} = \frac{1}{m_x} \left(\dot{X}_q \dot{q} + X_e + \dot{X}_u u + \dot{X}_w w + \left(\dot{X}_q - m_x W_e \right) q + X_{\delta_e} + X_{\delta_r} \right) \\ + X_1 \delta_1 - (mg - B) \sin(\theta_E + \theta_e) - m a_z \dot{q} \end{cases}$$

Normal Force

$$\begin{cases} \frac{dz}{dt} = w \\ \dot{w} = \frac{1}{m_z} \left(\dot{Z}_q \dot{q} + Z_e + \dot{Z}_u u + \dot{Z}_w w + \left(\dot{Z}_q + m_z U_e \right) q + Z_{\delta_e} \right) \\ + (mg - B) \cos \phi_E \cos(\theta_E + \theta_e) \\ + m a_z \dot{q} + Z_{\delta_r} + \dot{Z}_v v \end{cases}$$

Pitching Moment

$$\begin{cases} \frac{d\theta}{dt} = q \cos \phi_B - r \sin \phi_B \\ \dot{q} = \frac{1}{J_y} \left(\dot{M}_u \dot{u} + \dot{M}_w \dot{w} + M_e + \dot{M}_u u + \dot{M}_w w + \dot{M}_q q + M_{\delta_r} + M_{\delta_e} \right) \\ - m a_z \dot{u} + m a_x \dot{w} \\ - (m g a_z + B b_z) \cos(\theta_E + \theta_e) - (m g a_x + B b_x) \cos \phi_E \cos(\theta_E + \theta_e) \end{cases}$$

Side Force

$$\begin{cases} \frac{dy}{dt} = v \\ \dot{v} = \frac{1}{m_y} \left(\dot{Y}_p \dot{p} + \dot{Y}_r \dot{r} + Y_e + \dot{Y}_v v + \left(\dot{Y}_p + m_z W_e \right) p + \left(\dot{Y}_r - m_x U_e \right) r + Y_{\delta_r} \right) \\ + (mg - B) \sin \phi_E \cos(\theta_E + \theta_e) \\ + m a_z \dot{p} - m a_x \dot{r} + \dot{Y}_w w \end{cases}$$

Yawing Moment

$$\begin{cases} \frac{d\psi}{dt} = q \sin \phi_B \sec \theta_B + r \cos \phi_B \sec \theta_B \\ \dot{r} = \frac{1}{J_z} \left(J_{xz} \dot{p} + \dot{N}_v \dot{v} + N_e + \dot{N}_v v + \dot{N}_p p + \dot{N}_r r + N_{\delta_r} \right) \\ - m a_x \dot{v} + m a_z W_e p - m a_x U_e r \\ + (m g a_x + B b_x) \sin \phi_E \cos(\theta_E + \theta_e) \\ + N_{\delta_r} \end{cases}$$

Rolling Moment

$$\begin{cases} \frac{d\phi}{dt} = p + q \sin \phi_B \tan \theta_B + r \cos \phi_B \tan \theta_B \\ \dot{p} = \frac{1}{J_x} \left(J_{xz} \dot{r} + \dot{L}_v \dot{v} + L_e + \dot{L}_v v + \dot{L}_p p + \dot{L}_r r \right) \\ + m a_z \dot{v} - m a_x W_e p + m a_z U_e r \\ - (m g a_z + B b_z) \sin \phi_E \cos(\theta_E + \theta_e) \\ + L_{\delta_r} + L_{\delta_e} + N_{\delta_r} + \dot{L}_w \end{cases}$$

Examples of estimation of each coefficient and derivative in equation of motions

$$\begin{aligned} m_x &= m_{envelope} \times 2 \\ m_y &= m_{envelope} \times 2 \\ m_z &= m_{envelope} \times 2 \\ J_x &= I_{envelope} \times 2 + I_{device} \\ J_y &= J_x \\ J_z &= m_{envelope} \times r_{tube}^2 + 0.5 \times m_{device} \times r_{device}^2 \\ J_{xz} &= 0 \\ \dot{X}_u &= \rho_{air} \times S \times u \times C_D (measured) \\ \dot{Z}_u &= \rho_{air} \times S \times u \times C_L (measured) \\ \dot{M}_u &= \rho_{air} \times S \times u \times C_M (measured) \times l_{body} \\ &etc... \end{aligned}$$

Copyright Statement

The authors confirm that they, and/or their company or organization, hold copyright on all of the original material included in this paper. The authors also confirm that they have obtained permission, from the copyright holder of any third party material included in this paper, to publish it as part of their paper. The authors confirm that they give permission, or have obtained permission from the copyright holder of this paper, for the publication and distribution of this paper as part of the ICAS2010 proceedings or as individual off-prints from the proceedings.

Contact Author Email Address

If you want more information about this paper, please give us contact without consideration.
suefuku@gmail.com and hirayama@ynu.ac.jp